Influence of Converter and Inverter on Dynamic Behavior of the GMAW Process

A. R. Doodman Tipi[a]*, S. K. Hosseini Sani[a], N. Pariz[a]

[a] *Department of engineering, Ferdowsi University of Mashhad, Mashhad, Iran.*

ARTICLE INFO

Article history:

Received 18 Jun. 2014
Accepted 13 Oct. 2014
Available online 01 Dec. 2014

Keywords:

Dynamic modeling
GMAW process
Signal processing
Power supply

ABSTRACT

This paper investigates the dynamic behavior of Gas Metal Arc Welding (GMAW) process for two types of power supplies– inverter and rectifier-for short circuit transfer mode. The large ripples on the rectifier power source are able to perturb the metal transfer mode. In this experimental work some operating points in the short circuit mode have been selected using an automatic pipeline welding system, and the effects of both rectifier and inverter effects (as the power supplies) on the process have been illustrated. For small voltage and currents, the two power supplies effects are similar in the short circuit transfer mode. On the other hand, for larger voltage and current values, the responses will be different as the rectifier power supply produces more perturbations on the metal transfer. However, the process with the inverter has a more regular behavior and a more stable detachment.

1. Introduction

Either DC rectifier or DC inverter are usually used as the power supply in the GMAW process. In the previous studies, the power supply was simulated as a simple ideal source, i.e.a voltage source in series with an RL circuit. Consequently, the dynamic model of the GMAW process was derived using such a simple model of the power supplies. However, a real power supply has a complex behavior compared to such a simple and ideal model, due to its numerous nonlinear and complex parts, including the transformers, diode bridges, thyristors, IGBTs, inductances, and fire circuits. In a previous study [1], both inverter and rectifier were modeled with the characteristic equations and experimental and simulation results were compared. On the other hand, while the dynamic behavior of the process has been investigated in the literature for various transfer modes (short circuit, globular and spray) [2-7], there is almost no study about the influence of the power supplies on the dynamic behavior and detachment status.

In this research, some experimental tests are conducted to provide a better insight about the effects of the power supply on the process behavior in the short-circuit mode. The experimental setup is a professional automatic pipeline welding system and, as a result, the tests results are valid for all possible angles (0-180^{o}).

This paper is organized as follows. The GMAW system and its subsystems are modeled in Section 2 to investigate the effect of the

Corresponding author:
E-mail address: adoodman@gmail.com (Alireza Doodman).

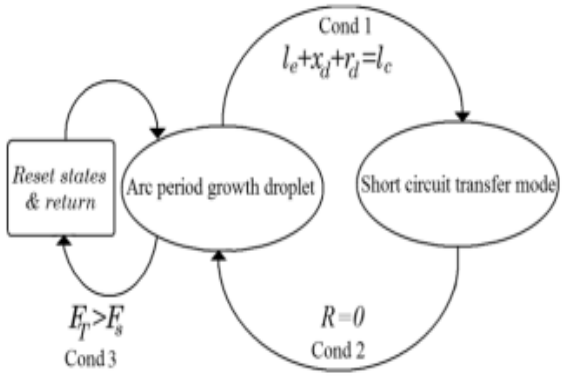

Fig. 1. Metal transfer working sketch to include three states of short circuit period, arc period and detaching event

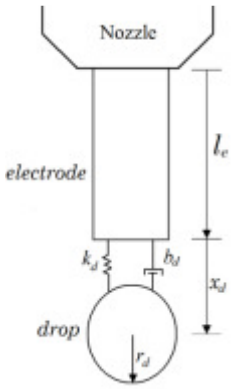

Fig. 2. Mass-spring-damper model for a molten drop during the arc period

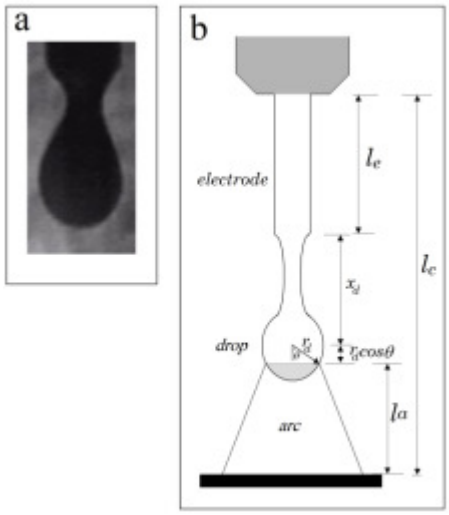

Fig. 3. A real picture of the drop and molten shape and electrode (a; reprinted from [14]). A schematic view of the arc length, electrode extension, and other distances (b)

inverter and rectifier power supplies on the GMAW dynamics. Experimental results on a test setup are presented in Section 3. Finally, the paper is concluded in Section 4.

2. Modeling

The metal transfer phenomenon in its general form, i.e. including both free flight and short circuit modes, can be seen as a hybrid system as shown in Fig. 1. In fact, it presents two continuous states [8] and a drop detachment criterion in the arc period. The first state occurs when the drop grows, while the second one happens when the electrode is in physical contact with the workpiece. The drop detachment is not a permanent state, but it happens during the detachment and some variables are being reset (in this time) and then the states immediately return to the arc period.

- *Condition 1*: The Contact-Tube to Workpiece Distance (CTWD) is inferior to the electrode extension plus droplet length.
- *Condition 2*: The molten metal bridge diameter is inferior to a threshold fixed by electrical and material laws.
- *Condition 3*: In the arc period, the surface tension of the drop (F_s) is inferior to the total force (F_T) that pulls the drop.

Automatic GMAW system consists of several subsystems with various dynamics. Both the terminal voltage of the power supply and the power cable are modeled by an equivalent RL circuit along with a voltage source [10, 29]:

$$L\frac{dI}{dt}+(R_s+k_2 l_e)I+V_a=V_t \quad [1]$$

The electrode extension is defined as the distance from the contact tube to the melting point of the electrode (see Fig. 3). The electrode extension is varied according to the melting speed, electrode speed and nozzle speed. The following equation represents the electrode extension dynamics [8].

$$\frac{dl_e}{dt}=v_e-v_m+v_c \quad [2]$$

The relationship between the melting speed (v_m) and welding current (I), is usually described by a parabolic model that considers two forms of the electrode heating (the arc heating and joule heating) [8-9].

Table 1. Symbols, parameters, and variables for simulation and experimental systems

Nomenclature	Symbol	Value (unit)
Output Resistance of power supply	R_s	$6.8\times10^{-3}(\Omega)$
Output Inductance of power supply & cable	L	170×10^{-6} (H)
Electrode extension	l_ω	(mm)
Arc length	l_a	(mm)
Welding Current	I	(A)
Contact tube voltage	V_f	(v)
Terminal voltage	V_t	(v)
Reference voltage	V_r	(v)
Average pressure in the bridge	P_{avg}	$(N.m^{-2})$
Bridge cylinder radius (conical shape)	R	(m)
Wire feed speed	v_e	$(m.s^{-1})$
Drop position	x_d	(m)
Density of the liquid electrode material	ρ_e	$7860(kg.m^{-3})$
Surface tension coefficient	γ	$1.3(N.m^{-1})$
Permeability of free space	μ_0	$1.25\times10^{-6}(kg.m.A^{-2}s^{-2})$
Bridge center distance from workpiece	h	(m)
The angle between the conducting zone and drop	θ	(deg)
Drop radius	r_d	(m)
Gravity coefficient	g	$9.8\ (m.s^{-2})$

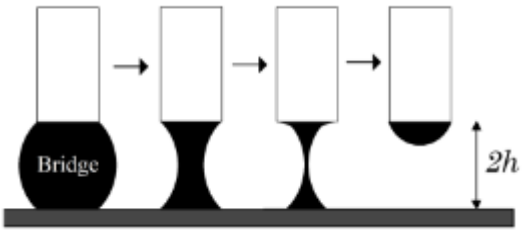

Fig. 4. The bridge shape during the short circuit time

$$v_m = k_1 I + k_2 l_e I^2 \quad [3]$$

The arc can be modeled through some relationships between the total arc voltage, welding current, and arc length. Eq. (4) describes the arc equation using Ayrton's formula [2].

$$V_a = V_0 + k_3 I + k_4 l_a + k_5 I l_a \quad [4]$$

k_1, k_2, k_3, k_4 and k_5 in (3) and (4) denote the constants which depend on the type and size of the electrode and the shielding gas [4, 8]. These values are experimentally computed (Table 1).

Basically, drop detachment occurs when the surface tension is exceeded by other drop affecting forces [4]. Eq. (5) is a mass-spring-damper model to describe the pendant drop dynamic (illustrated in Fig. 2).

$$m_d \ddot{x}_d = F_T - b_d \dot{x}_d - k_d x_d \quad [5]$$

The drop mass (m_d), varies in time. Drop mass variation depends on the melting rate. This can be expressed by:

$$\frac{dm_d}{dt} = M_R \rho_e \quad [6]$$

Notice that the melting rate (melting volume per time) can be expressed by the melting speed (length of the melting electrode per unit time), as stated below:

$$M_R = \pi r_e^2 v_m \quad [7]$$

In (5), there are some forces which affect the drop detachment, including the gravity, electromagnetic, aerodynamic, and momentum forces [4,10-11]. Hence, the total force (F_T) can be described as below:

$$F_T = F_g + F_{em} + F_d + F_m \quad [8]$$

The gravity vector force is a function of the welding angle; so, the gravitational force changes according to the welding angle. Therefore, F_g can be stated according to Eq. (9) [6],

$$F_g = m_d g \cos(\varphi) \quad [9]$$

Eq. (10) represents the electromagnetic

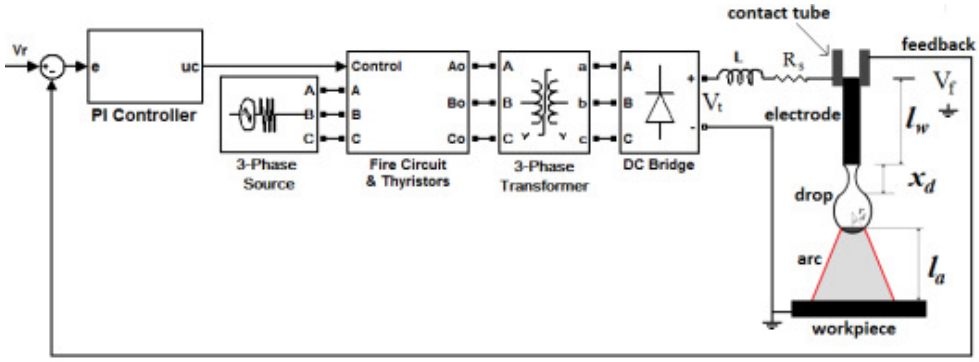

Fig. 5. Rectifier block diagram as the power supply in GMAW process

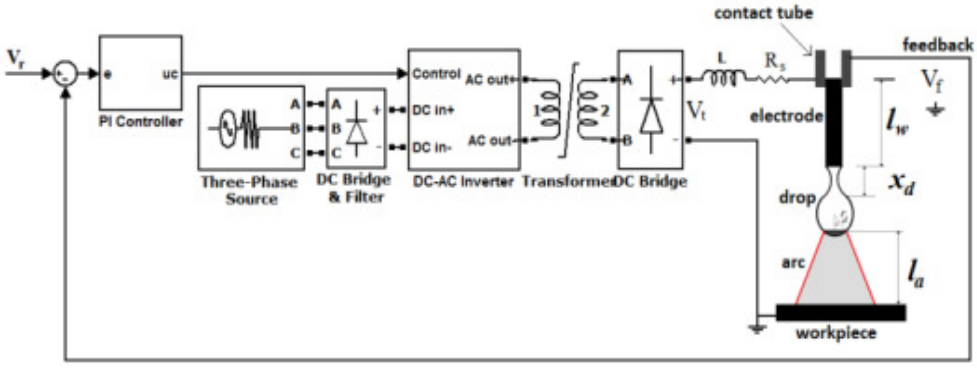

Fig. 6. Schematic diagram for inverter as the power supply in GMAW process

force. The welding current, electrode radius, drop radius, and cross angle between the drop and arc (θ), are used to calculate the electromagnetic force [11],

$$F_{em}=\frac{\mu_0 I^2}{4\pi}\left[\ln\left(\frac{r_d\sin(\theta)}{r_e}\right)-\frac{1}{4}-\frac{1}{1-\cos(\theta)}+\frac{2}{(1-\cos(\theta))^2}\ln\left(\frac{2}{1+\cos(\theta)}\right)\right] \quad [10]$$

The surface tension is computed by Eq. 11:

$$F_s=2\pi r_e\gamma \quad [11]$$

In this work the Static Force Balance Model (SFBM) is used to obtain the detachment condition [4, 11]. Hence, the drop is detached if the following inequality is fulfilled:

$$F_T>F_s \quad [12]$$

The volume of the liquid material, left on the electrode after the detachment is given by Eq. 13 [9].

$$V_d=\frac{m_d}{2\rho_e}\left(\frac{1}{1+e^{-100v_d}}+1\right) \quad [13]$$

The robot angle is considered as an augmented state variable:

$$\frac{d\varphi}{dt}=\frac{1}{R_p}v_T \quad [14]$$

Eq. 15 presents the relationship between the stick out, CTWD, arc length, the drop radius, and the cross zone angle (see Fig. 3) [6].

$$l_a=l_c-l_e-x_d-r_d\cos(\theta) \quad [15]$$

In the short-circuit mode, the detachment does not occur during the arc period since the detaching force is smaller than the tension force in this period. Also, distance between the drop and the workpiece will be small before the short circuit happens. In the short circuit period, the current rises and the drop detaches [5-6]. In this period, a bridge shape is created between the electrode and the workpiece. Fig. 4 shows the bridge from the start to the end of the short circuit event.

The average pressure [9] on the cross section of the bridge center is derived as follows:

$$P_{avg}=\frac{\mu_0 I^2}{8\pi^2 R^2}+\frac{\gamma}{R} \quad [16]$$

The flow velocity [10] at the contact between the electrode neck and the pool surface can be modified to consider the effect of the angle on the gravity force:

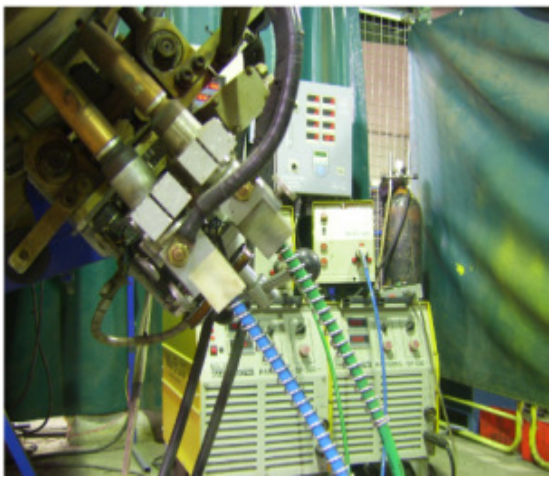

Fig. 7. The welding system with the rectifiers used in the experiments

$$v_f = \sqrt{\frac{2}{\rho_e}\left(P_{avg} + \rho_e g h \cos(\theta)\right)} \quad [17]$$

2. 1. Rectifier structure

A rectifier power supply includes a three-phase voltage source, thyristors and fire circuits, three-phase transformer, DC bridge, feedback line, comparator, and controller. Fig. 5 shows the schematic diagram of a rectifier power supply and its control loop. The close loop control adjusts the feedback voltage based on the reference value [1].

2. 2. Inverter structure

Inverter, as a power supply, includes a three-phase line connected to a six-pulse DC bridge. The bridge's output is fed to the inverter pole and the output of the inverter is a high-frequency wave, passing through a high frequency transformer and a DC bridge. The output voltage level is regulated by the control signal to adjust the DC output level according the reference voltage (V_r). Fig. 6 shows the schematic diagram of an inverter power supply. Modeling and characteristic equations for these power supplies have been derived and simulated in the previous work [1].

The main difference between the inverter and rectifier is the large low-frequency ripples observed in the voltage and current wave forms of the rectifier system. This ripple influences the detachment and dynamic behavior of the process.

3. Experimental results

3. 1. Experimental setup

The test system used in the experiments is commercial system, named "POOYA" system, and is manufactured by Novin Sazan Co. (Fig. 7). This system is an industrial automatic GMAW pipeline system [11]. The system parameters, constants, and symbols are listed in Table 1. The parameters values in Table 1 are valid for steel wire with 1mm diameter and 82%Ar + 18%CO_2 shielding gas. Pipe thickness and diameter are 20.6mm and 32inch, respectively. "GAM-ELECTRIC SP-500"isemployed as the DC rectifier power supply; also, "MILLER XL-350" has been used as inverter power supply. The experimental tests include three cases of small, large and huge operating points.

3. 2. Small operating point (test 1)

In this case, the amplitude of voltage and current are small in the short-circuit region. If the operating point is sufficiently far from the globular region, the ripples and disturbances are not able to perturb the detachment. Therefore, the drop detaching is in the short-circuit region with a regular detachment frequency.

The welding robot turns around the pipe 180 degrees. Hence the illustrated detachment frequency in Fig. 9 is for the whole angle ranges (0 to 180°).

3.2.1. Test1-Rectifier system

The operating point has been selected as:

$V_r = 19v \qquad I = 140A \qquad v_e = 100mm/\sec$

For this operating point, the robot moves from top to the bottom of the pipe for 192 seconds. Because of the small magnitude of the voltage and current, the large inherent ripples of the rectifier are not able to perturb the detaching yet.

Fig. 8 shows the welding voltage and current within 0.3 sec, and Fig. 9 illustrates the time-frequency representation for the welding voltage of the rectifier system. The detaching frequency lies in the 20-30 Hz frequency band.

3.2.2. Test 1-Inverter system

In this experiment, the pervious operating point

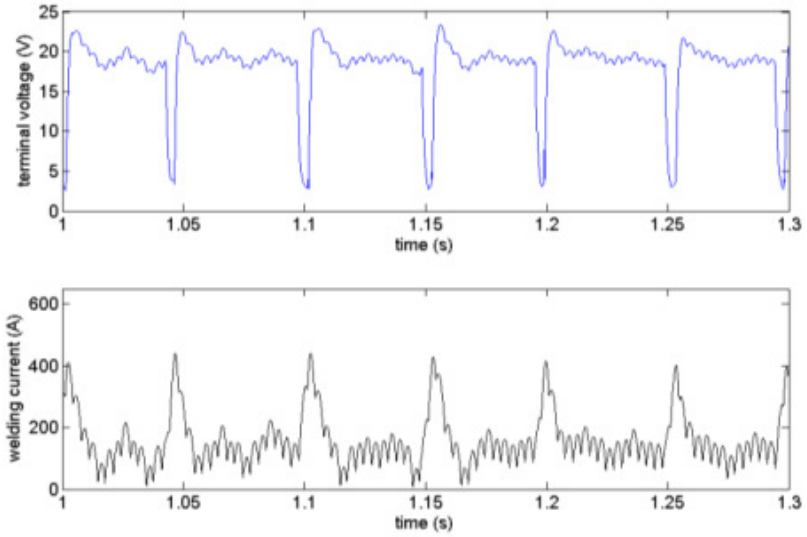

Fig. 8. A window time -0.3 seconds- of terminal voltage and welding current (test1-rectifier power source)

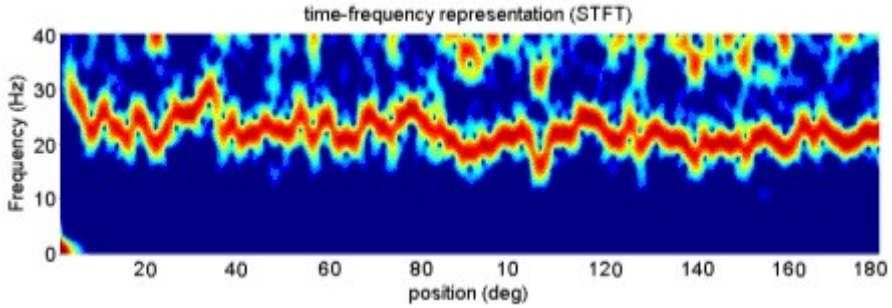

Fig. 9. Time-frequency representation of terminal voltage in small operating point (test 1-rectifier power source)

Is used for the welding system with the inverter power supply. Taking Figs. 10 and 11 into account, the responses are similar to the rectifier experiments except for the low frequency ripples in the previous test. Therefore, the detaching frequency bands are almost identical for the two systems.

3. 3. Large operating point (test 2)

If the voltage and current are larger, the transfer region will be close to the globular mode. Under such a condition, the ripples and disturbances are able to influence the metal transfer mode, particularly in the case oft he rectifier power supply as there are large ripples in the current and voltage wave forms. The next experimental test illustrates the influences of the ripples.

3.3.1. Test 2-Rectifier system

The border between the short circuit and globular model is known as the mixed region [6]. When the voltage and current increase the transfer mode approaches the mixed mode. In this case the ripples have a stronger effect on the detaching.

The operating points for test 3 are as follows:

$V_r = 20.5v \qquad I = 200A \qquad v_e = 133mm/\sec$

The test results for this case are shown in Figs. 12 and 13. The short-circuit events are irregular due to the mixed mode detaching and the ripple's effects. The time-frequency representation in Fig. 11 demonstrates the short-circuit events for the majority of the positions (0 to 180°).

3.3.2. Test 2-Inverter system

The operating point in this test has been selected similar to test 3. Moreover, in this test the inverter is used as the power supply. The results for this experimental test are depicted in Figs. 14 and 15. Based on these figures, the detachment is still regular in contrast to the

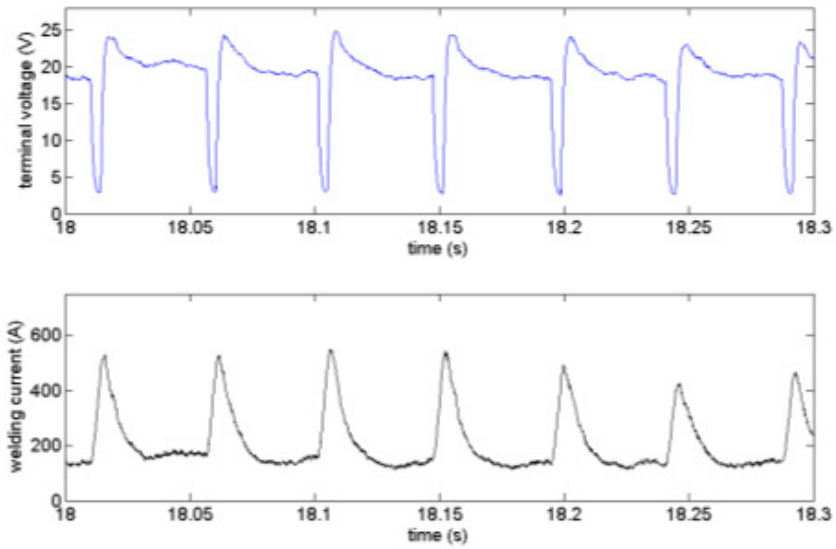

Fig. 10. A window time -0.3 second- of terminal voltage and welding current (test1-inverter power source)

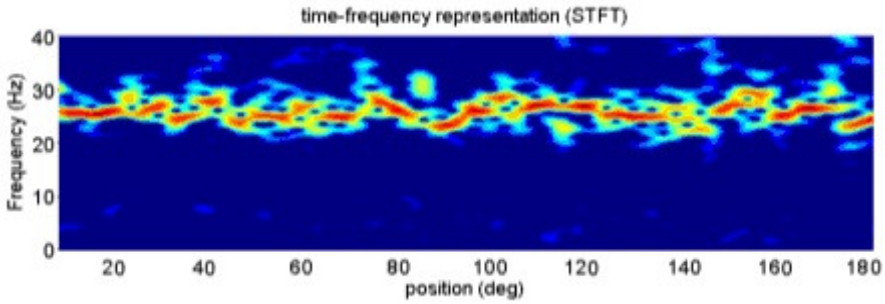

Fig. 11. Time frequency representation for terminal voltage (test1-inverter power source)

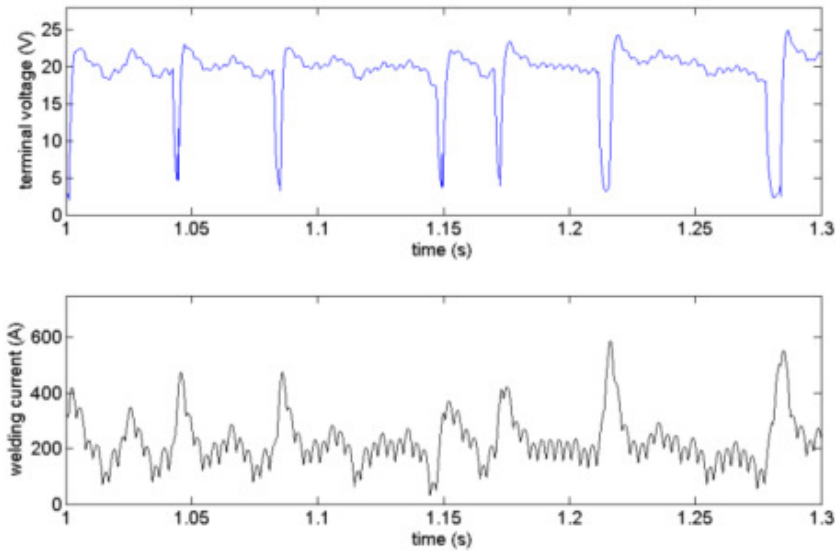

Fig. 12. A window time -0.3 second- of terminal voltage and welding current in (test2-rectifier power source)

pervious test results obtained for the rectifier power supply. Indeed, these results confirm the narrow mixed transfer region for the inverter as the power supply in the GMAW process thanks to the very smaller ripples compared to the rectifier power supply.

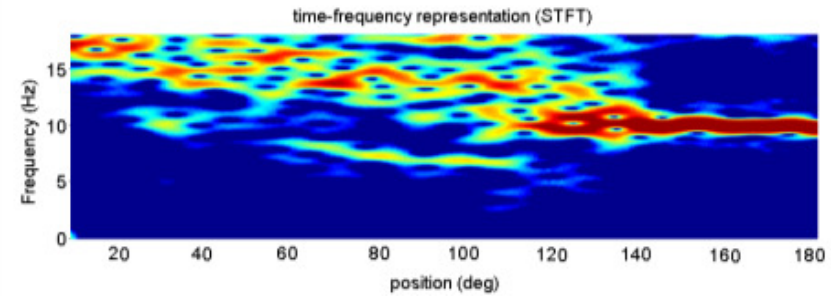

Fig. 13. Time frequency representation for terminal voltage in (test2-rectifier power source)

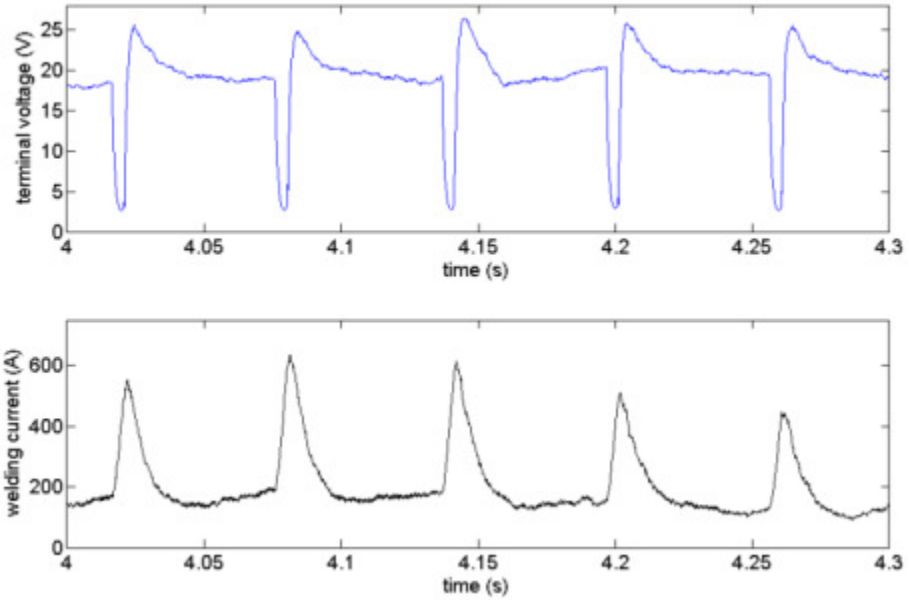

Fig. 14. A window time -0.3 second- of terminal voltage and welding current (test2-inverter power source)

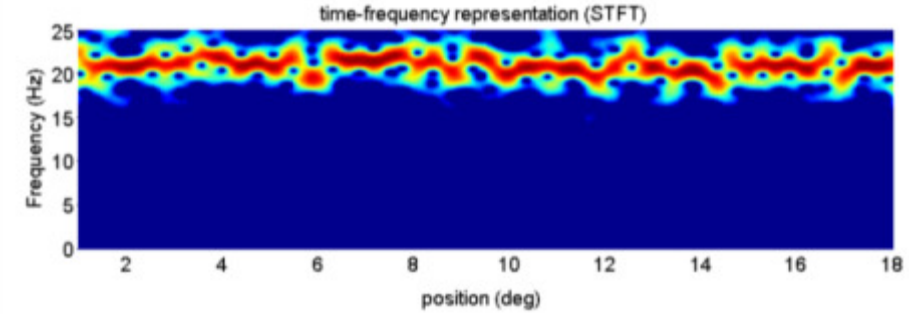

Fig. 15. Time frequency representation for terminal voltage (test2-inverter power source)

3. 4. Globular mode (test 3)

3.4.1. Test 3-Rectifier

In the third case, the value of voltage further increases to achieve the following operating point:

$V_r = 21.5v \qquad I = 200A \qquad v_e = 133mm/\sec$

For these parameters, the transfer region is in globular mode approximately. With the rectifier power supply, a window time of 0.6 seconds of the voltage and current is shown in Fig. 16. Due to the ripples effects, the short circuit events are seen in the results and the detachment is not regular as well.

3.4.2. Test 3-Inverter

Fig. 17 shows the test results obtained for the

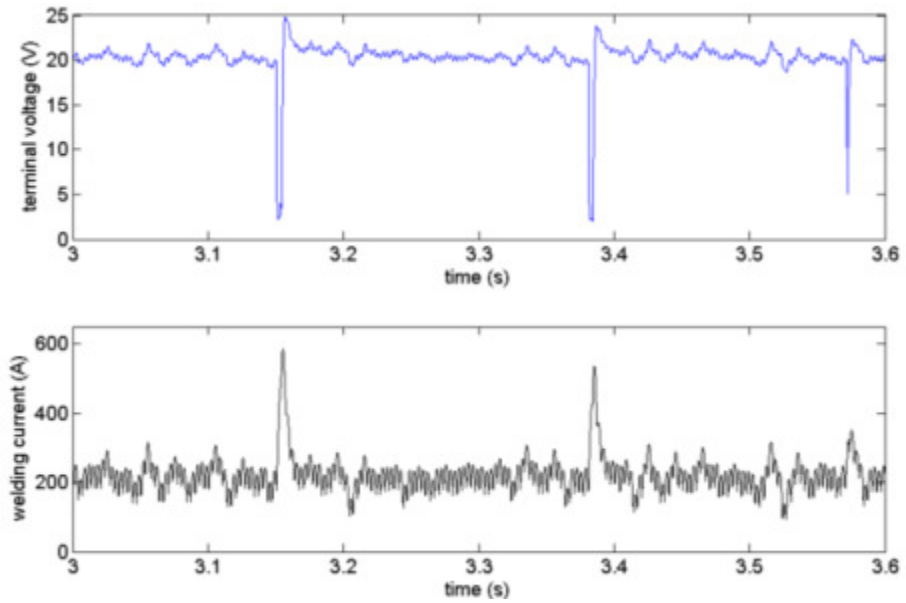

Fig. 16. A window time -0.6 second- of terminal voltage and welding current (test3-rectifier power source)

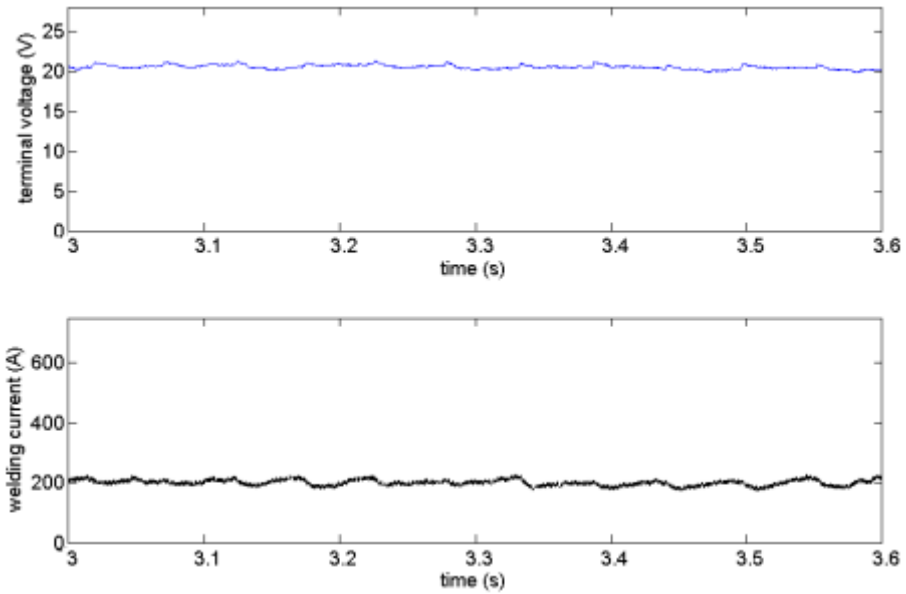

Fig. 17. A window time -0.6 second- of terminal voltage and welding current (test3-inverter power source)

inverter power supply (with test 3 parameters). The transfer mode is entirely in the globular mode and the short circuit-events are not observed in the responses as there are small ripples and disturbances in the inverter output waveforms.

4. Conclusion

In this work, some experimental tests were performed to compare the metal transfer in the rectifier and inverter as power supplies for the GMAW process. The experimental setup was an automatic pipeline system and therefore the system dynamics was studied for the entire range of angles (from 0 to 180°).

It was shown that due to the large amplitude of the ripples in the rectifier power supply, the metal transfer is more perturbed. When a rectifier is used as power supply, the mixed transfer mode (composed of short-circuit and globular transfer modes) has a wide range.

On the other hand, when the inverter power

supply is used, the process responses are more stable and the drop detachment in the experimental results is more regular. In particular, in the case of larger voltage and currents (demonstrated in tests 2 and 3), the inverter is preferred to the rectifier system. Moreover, these results are valid for the short-circuit mode as the experiments were carried out only in this region. The globular and spray modes will be studied in future works by the authors. The experimental results, presented in this paper, can be usefully employed in choosing the suitable type of the power supply for the manual or automatic GMAW systems.

References

1. A. R. Doodman Tipi,S. K. Hosseinisani, N. Pariz, "Improving the dynamic metal transfer model of gas metal arc welding (GMAW) process", Int. J. Adv. Manuf. Technol (*in press*).

2. S. K. Choi, C. D. Yoo, Y. S. Kim, "Dynamic simulation of metal transfer in GMAW - Part 1: globular and spray transfer modes", Weld. J., Vol. 77, 1998, pp. 38-44.
3. K. L. Moore, D. S. Naidu, R. Yender, J. Tyler, "Gas metal arc welding control: part I – modeling and analysis", Nonlin.Anal., theory meth. & applic., Vol. 30, 1997, pp. 3101-3111.
4. J. S. Thomsen, Advanced control methods for optimization of arc welding. Ph.D. Thesis, Aalborg University, Denmark, 2004.
5. S. K. Choi, S. H. Ko, C. D. Yoo, Y. S. Kim, "Dynamic simulation of metal transfer in GMAW-Part 2: short circuiting transfer mode", Weld. J., *Vol.* 77, 1998,pp. 45-52.
6. J. H. Cho, J. Y. Le, C. D. Yoo, "Simulation of dynamic behavior in a GMAW system", Weld. J., Vol. 80, 2001, pp. 239-246.
7. A. R. Doodman Tipi, "The study on the drop detachment for automatic pipeline GMAW system: short circuit mode", Int. J. Adv. Manuf. Technol., Vol. 50, 2010, pp. 149-161.
8. J. P. Planckaert, E. H. Djermoun, D. Bri, F. Briand, F. P. Richard, "Droplet features extra condition with a dynamic active contour for MIG/MAG welding modeling", IProc. 18th international conferenceon system Engineering (ICSE), UK, 2006.
9. J. F. Lancaster, The physics of welding. 2nd edition, Pergamon publication, US, 1986.
10. A. R. DoodmanTipi, "The study on the drop detachment for automatic pipeline GMAW system: free flight mode", Int. J. Adv. Manuf. Technol., Vol. 50, 2010,pp. 137-147.
11. A. R. Doodman Tipi, "Neutralizing the effect of the Angle Variations on the Drop Detachment in Automatic Pipeline GMAW System", Int. J. Adv. Manuf. Technol., Vol. 54, 2011, pp. 123-137.
12. A. R. Doodman Tipi, S. A. Mortazavi, "A new adaptive method (AF-PID) presentation with implementation in the automatic welding robot", Proc. IEEE/ASME International Conferenceon Mechatronic and Embedded SystemApplication (MESA), China. 2008.